Astronomy & Astrophysics manuscript no. 3927 February 5, 2008
(DOI: will be inserted by hand later)

Photodissociation of organic molecules in star-forming regions II: Acetic acid

S. Pilling[1,2], A. C. F. Santos[3], and H. M. Boechat-Roberty[1]

[1] Observatório do Valongo, Universidade Federal do Rio de Janeiro, Ladeira Pedro Antônio 43, CEP 20080-090, Rio de Janeiro, RJ, Brazil.
[2] Instituto de Química, Universidade Federal do Rio de Janeiro, Ilha do Fundão, CEP 21949-900, Rio de Janeiro, RJ, Brazil
[3] Instituto de Física, Universidade Federal do Rio de Janeiro, Caixa Postal 68528, CEP 21941-972, Rio de Janeiro, RJ, Brazil

Received / Accepted

Abstract. Fragments from organic molecule dissociation (such as reactive ions and radicals) can form interstellar complex molecules like amino acids. The goal of this work is to experimentally study photoionization and photodissociation processes of acetic acid (CH_3COOH), a glycine (NH_2CH_2COOH) precursor molecule, by soft X-ray photons. The measurements were taken at the Brazilian Synchrotron Light Laboratory (LNLS), employing soft X-ray photons from a toroidal grating monochromator (TGM) beamline (100 - 310 eV). Mass spectra were obtained using the photoelectron photoion coincidence (PEPICO) method. Kinetic energy distribution and abundances for each ionic fragment have been obtained from the analysis of the corresponding peak shapes in the mass spectra. Absolute photoionization and photodissociation cross sections were also determined. We have found, among the channels leading to ionization, that only 4-6% of CH_3COOH survive the strong ionization field. CH_3CO^+, $COOH^+$ and CH_3^+ ions are the main fragments, and the presence of the former may indicate that the production-destruction process of acetic acid in hot molecular cores (HMCs) could decrease the H_2O abundance since the net result of this process converts H_2O into OH + H^+. The $COOH^+$ ion plays an important role in ion-molecule reactions to form large biomolecules like glycine.

Key words. CH_3COOH – Photoionization – Photodissociation – X-rays – Astrochemistry

1. Introduction

Acetic acid (CH_3COOH) has been detected toward various astrophysical regions, including hot molecular cores (HMCs) associated with low- and high-mass star-forming regions (Remijan et al. 2002, 2003, 2004; Cazaux et al. 2003; Mehringer et al. 1997; Wotten et al. 1992 and Wlodarczak & Demaiso 1988) and in comets (Crovisier et al. 1999, 2004). In these environments the radiation field can promote several photophysical and photochemical processes, including the photodissociation. The products of organic molecule dissociation (such as reactive ions and radicals) can form interstellar complex molecules like long carbon chain molecules and amino acids.

The simplest amino acid, glycine (NH_2CH_2COOH), was recently detected in the molecular clouds SgrB2, Orion KL and W51 (Kuan et al. 2003, 2004), although this result was questioned by Snyder et al. (2005). In these objects, precursor molecules like ammonia (NH_3), methylamine (CH_3NH_2), formic acid (HCOOH) and acetic acid have been observed (Nummelin et al. 2000; Turner 1991 and Sutton et al. 1985). Liu et al. (2002) pointed out the importance of performing studies on carboxyl acids since they share common structural elements with biologically important species such as amino acids.

Sgr B2, Orion KL and W51 are massive star-forming regions where the presence of widespread UV and X-ray fields could trigger the formation of photodissociation regions (PDRs). X-ray photons are capable of traversing large column densities of gas before being absorbed. X-ray-dominated regions (XDRs) in the interface between the ionized gas and the self-shielded neutral layers could influence the selective heating of the molecular gas. The complexity of these regions possibly allows a combination of different scenarios and excitation mechanisms to coexist(Goicoechea et al. 2004).

The formation of interstellar acetic acid occurs both in the gas phase and on grain surfaces. Huntress & Mitchell (1979) proposed a radiative association mechanism followed by dissociative recombination with an electron in the gas-phase:

$$CH_3CO^+ + H_2O \longrightarrow CH_3COOH_2^+ \xrightarrow{e^-} CH_3COOH + H. \quad (1)$$

Ehrenfreund & Charnley (2000) have proposed a warm gas-phase route in which reactions with protonated methanol ($CH_3OH_2^+$) and formic acid, evaporated from grain surfaces, can result in CH_3COOH formation.

Send offprint requests to: S. Pilling,
e-mail: pilling@ov.ufrj.br

Sorrel (2001) has proposed that accretion of gas-phase H, O, OH, H_2O, CH_4, NH_3 and CO onto dust grains sets up a carbon-oxygen-nitrogen chemistry in the grain. As a consequence, a high concentration of free OH, CH_3 and NH_2 radicals is created in the grain mantle mainly by photolysis. Once these radicals are created, they remain frozen in position until the grains heat up. As this occurs, the radicals become mobile and undergo chemical reactions amongst themselves and with other adsorbed molecules to produce complex organic molecules including CH_3COOH. Remijan et al. (2002) pointed out the importance of grain-surface chemistry to form acetic acid, since the location of acetic acid emission is nearly coincident with the emission from other large molecular species formed by grain-surface chemistry in HMCs.

Two isomers of acetic acid have also been detected toward HMC, associated with star-forming regions, methyl formate ($HCOOCH_3$) and glycolaldehyde (CH_2OHCHO). Hollis et al. (2001) have measured the column density of both isomers in the Sgr B2 (LMH) source near the galactic center and the relative abundances were quite different, about 1:26:0.5 (CH_3COOH:$HCOOCH_3$:CH_2OHCHO). This suggests a different pathway of formation and/or different stability against the radiation field, which will be discussed in a future publication.

Remijan et al. (2004) have proposed that CH_3COOH formation seems to favor HMCs with well-mixed N and O, despite the fact that CH_3COOH does not contain an N atom. If this is proved to be true, this is an important constraint on CH_3COOH formation and, possibly, other structurally similar biomolecules. Despite the differences in molecular structure and chemical formation mechanisms, methyl cyanide, ethyl cyanide (CH_3CH_2CN) and acetic acid are found to have similar abundances toward the W51 e1 and e2 sources.

The photodissociation of acetic acid has been studied experimentally and theoretically in the ultraviolet region (Bernstein et al. 2004; Maçôas et al. 2004, Fang et al. 2002; Naik et al. 2001; Hunnicutt et al. 1989; Blake & Jackson 1969). However, despite some photoabsorption studies in the X-ray range (Robin et al. 1998 and references therein) there are no studies focusing on the photodissociation pathways due to soft X-rays. The present work aims to examine the photoionization and photodissociation of acetic acid by soft X-rays, from 100 eV up to 310 eV, including the energies around the carbon K edge (~ 290 eV).

2. Experimental setup

The experiment was performed at the Brazilian Synchrotron Light Laboratory (LNLS) in Campinas, São Paulo, Brazil. Soft X-rays photons (~ 10^{12} photons/s) from a toroidal grating monochromator (TGM) beamline (100-310 eV), perpendicularly intersect the gas sample inside a high vacuum chamber. The gas needle was kept at ground potential. The emergent photon beam flux was recorded by a light sensitive diode. The sample was bought commercially from Sigma-Aldrich with purity greate than 99.5%. No further purification was performed other than degassing the liquid sample by multiple freeze-pump-thaw cycles before admitting the vapor into the chamber.

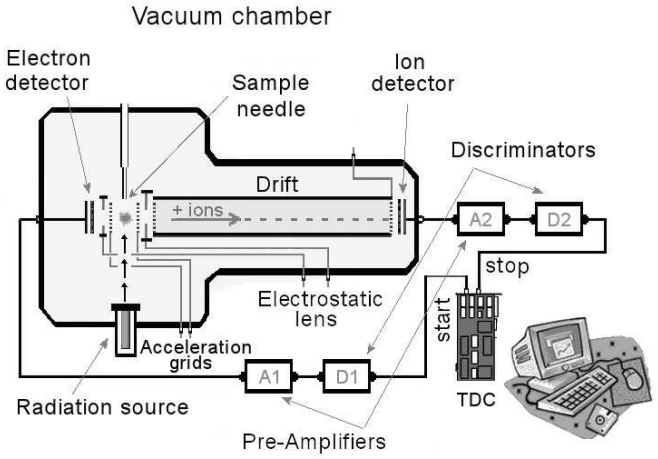

Fig. 1. Schematic diagram of the time of flight mass spectrometer inside the experimental vacuum chamber and the associated electronics.

Conventional time-of-flight mass spectra (TOF-MS) were obtained using the correlation between one Photoelectron and a Photoion Coincidence (PEPICO). The ionized recoil fragments produced by the interaction with the photon beam were accelerated by a two-stage electric field and detected by two micro-channel plate detectors in a chevron configuration, after mass-to-charge (m/q) analysis by a time-of-flight mass spectrometer (297 mm long). They produced up to three stop signals to a time-to-digital converter (TDC) started by the signal from one of the electrons accelerated in the opposite direction and recorded without energy analysis by two micro-channel plate detectors. A schematic diagram of the time of flight spectrometer inside the experimental vacuum chamber is shown in Figure 1, where A1 and A2 are the pre-amplifiers and D1 and D2 are the discriminators. The connection to the time-to-digital converter is also shown. Besides PEPICO spectra, other two kinds of coincidence mass spectra were obtained simultaneously, PE2PICO spectra (PhotoElectron Photoion Photoion Coincidence) and PE3PICO spectra (PhotoElectron Photoion Photoion Photoion Coincidence), which will be presented in a future publication. These spectra have ions coming from double and triple ionization processes, respectively, that arrive coincidentally with photoelectrons. Of all signals received by the detectors only about 10% come from PE2PICO and 1% from PE3PICO spectra, reflecting that the majority contribution is indeed due to single event coincidence. Nonetheless, PEPICO, PE2PICO and PE3PICO signals were taken into account for normalization purposes. Recoil ion and ejected electron detection efficiencies of 0.23 and 0.04, respectively, were assumed. In addition, we adopted the efficiencies of 0.54 and 0.78 to detect at least one of the photoelectrons from double ionization and triple ionization events, respectively (Cardoso 2001).

The first stage of the electric field (708 V/ cm) consists of a plate-grid system crossed at the center by the photon beam . The TOF-MS was designed to have a maximized efficiency for ions with energies up to 30 eV. The secondary electrons produced in the ionization region are focused by an electrostatic lens polarizing the electron grid with 800 V, designed to fo-

cus electrons at the center of the micro-channel plate detector. Negative ions may also be produced and detected, but the corresponding cross-sections are negligible.

The base pressure in the vacuum chamber was in the 10^{-8} Torr range. During the experiment the chamber pressure was maintained below 10^{-5} Torr. The pressure at the interaction region (volume defined by the gas beam and the photon beam intersection) was estimated to be $\sim$ 1 Torr (10^{16} mols cm−3). The measurements were made at room temperature.

3. Results and discussion

Figure 2 shows the mass spectrum of acetic acid obtained at photon energy of 288.3 eV. The C1s$\rightarrow$ π^* resonance energy from C=O bond is 288.6 eV (Robin et al 1988). We can see the methyl fragment group (mass from 12 to 15 a.m.u), the C_2 group (24 to 27 a.m.u), the HCO group (28 to 31 a.m.u) and the CCO group (40 to 44 a.m.u). The carbon dioxide ion (CO_2^+) is also produced. At mass 45 a.m.u. we see the carboxyl ion ($COOH^+$). $^{13}CH_3COOH^+$ (or $CH_3^{13}COOH^+$) is also seen.

The ions with the largest yields are the ionized acetyl radical (CH_3CO^+), ionized methyl (CH_3^+) and the ionized carboxyl radical ($COOH^+$). The first two may be interpreted as a result of neutral OH and COOH liberation, due to the bond rupture near the carbonyl in the dissociation process.

The CH_3^+ and $COOH^+$ fragments present similar relative partial yield which may indicate that the molecular dissociation due to photoionization of the C1s inner shell-electron at 288.3 eV does not have a preferential carbon atom target. In this case, both molecular fragments could retain the core hole (charge). However, as we can see in Figure 3 and in Table 1, there was a small enhancement ($\leq$ 20%) in the production of $COOH^+$ with respect to CH_3^+ in the photon energy range of 288 to 300 eV. This behavior may be associated with some instabilities of CH_3^+ ion leading to subsequence fragmentation and/or charge resonance in the $COOH^+$ ion, increasing its stability.

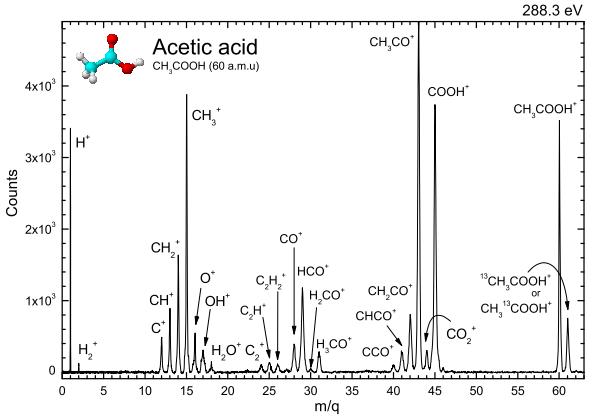

Fig. 2. Time-of-flight mass spectra of acetic acid molecule recorded at 288.3 eV.

Figure 3 shows the partial ion yields (PIY) for the most significant outcomes (CH_3CO^+, $COOH^+$, H^+ and CH_3^+) in the

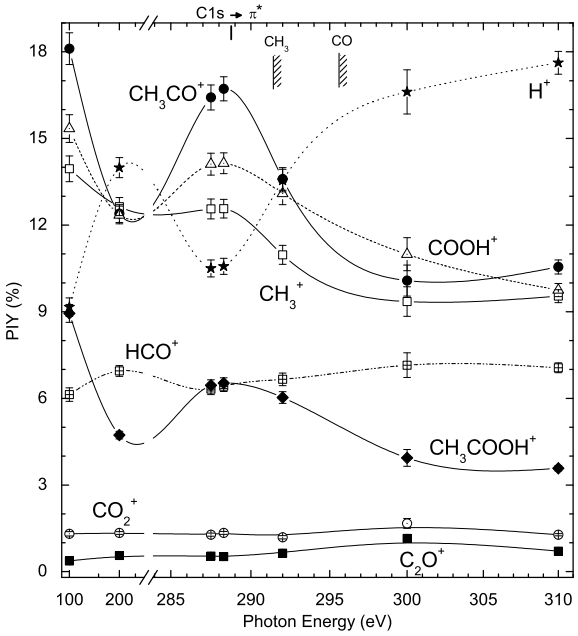

Fig. 3. Partial ion yield (PIY) of some PEPICO fragments of CH_3COOH molecule as a function of photon energy.

acetic acid dissociation in 100-310 eV photon energy range. The yields of some minor products like HCO^+, CH_3COOH^+, CO_2^+ and C_2O^+ are also shown. A clear bump can be seen in the fractions of CH_3CO^+, $COOH^+$, CH_3^+ and CH_3COOH^+ near the C1s resonance and decreasing to higher photon energies. The HCO^+ and H^+ fragments show a distinct behavior and also exhibit a gradual increase toward higher energies which indicates that these ions are preferentially formed after the normal Auger decay. The C_2O^+ (0.9%) and CO_2^+ (1.3%) fragments do not show any clear energy dependence. The C1s resonance and the ionization potential of each carbon are also indicated. The statistical uncertainties are below 10%.

In Figure 4 we compared the partial ion yield in soft X-rays (292 eV) obtained at LNLS and UV (by 70 eV electrons)[1] from NIST[2]. The molecular ion CH_3COOH^+ is more destroyed by soft X-rays than by UV photons, as expected. The partial ion yields of several fragments are also different in X-ray and in UV fields, for example, the enhancement of $COOH^+$ and CH_3CO^+ produced by UV radiation. The opposite occurs with HCO^+ and all lower mass ions, which seem to be more efficiently produced by X-ray photons.

Practically no production of $HCOOH^+$ (formic acid ion) has been identified in the fragmentation by soft X-rays and, while UV photons produce only a small amount of this ion, as we can see in Figure 3 and 4. As was noted before, the CO_2^+ and the C_2O^+ yields remain unchanged in the UV-X-ray pho-

[1] The effect of 70 eV electrons is very similar to 21.21 eV (He I Lamp) photons in both cases the main ionization occurs in valence shells (see discussion in Lago et al. 2004)

[2] National Institute of Standards and Technology http://webbook.nist.gov/chemistry/

ton energy range. The same applies to H_2CO^+ (formaldehyde) despite the extremely low yield (Figure 4).

The largest production of ions due to the photodissociation by soft X-ray photons near the C1s resonance energy is for CH_3CO^+, followed by $COOH^+$, CH_3^+ and H^+. The former, as mentioned before, was suggested by Huntress & Mitchell (1979) to be the main precursor of acetic acid together with the water molecule. Therefore, the continuous formation-destruction cycle of acetic acid could act as a catalytic agent converting water molecules in OH + H or (O + 2H) and possibly promoting a reduction in the local H_2O abundance. For higher photon energies, as we can see in Figure 3, the proton production is the major outcome.

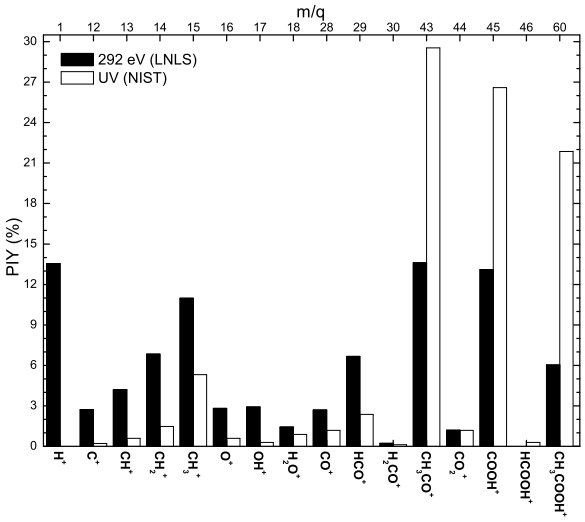

Fig. 4. Comparison of partial ion yield (PIY) of acetic acid fragments in soft X-ray and UV radiation.

The carboxyl radical, as has been discussed by several authors (Woon 2002, Largo et al. 2004 and Mendonza et al. 2004), plays an important role in the formation of large biomolecules including amino acids. Its ionic counterpart was one of the most ionic products released from the photodissociation of acetic acid by a moderate/strong ionizing photon field. This may suggest that never though acetic acid undergoes considerable photodissociation in star-forming region, it could still produce glycine and other carboxylated biomolecules via barrier-free ion-molecule reactions involving some of its reactant fragments like $COOH^+$.

3.1. Kinetic energy release (heating) of the ionic fragments

Several authors have recently focused on the pathway of formation of biomolecules present in the star-forming region and other gaseous-dusty astronomical media (Largo 2004, Woon 2002, and references therein). Despite the success of ab initio theoretical calculations, the endothermic ion-molecule reactions have been neglected and only exothermic reactions have been accepted as a viable mechanism. However, with the knowledge of the kinetic energy (or at least with its value range) of some radical and ionic fragments, some endothermic ion-molecule reactions could be likely and, in extreme situations, or even become more efficient than exothermic reactions.

We have determined the kinetic energy of all cationic fragments from the photodissociation of acetic acid. The present time-of flight spectrometer was designed to fulfil the Wiley-McLaren conditions for space focusing (Wiley & McLaren 1955). Within the space focusing conditions, the observed broadening of peaks in spectra is mainly due to kinetic energy release of fragments. Considering that the electric field in the interaction region is uniform, we can determine the released energy in the fragmentation process (U_0) from each peak width used by Simon et al. (1991), Hansen et al. (1998) and Santos, Lucas & de Souza (2001)

$$U_0 = \left(\frac{qE\Delta t}{2}\right)^2 \frac{1}{2m} \qquad (2)$$

where q is the ion fragment charge, E the electric field in the interaction region, m is the mass of the fragment, and Δt is the time peak width (FWHM) taken from PEPICO spectra. In order to test the above equation we have measured the argon mass spectrum under the same conditions.

The calculated values for kinetic energy release (U_0) for acetic acid fragmentation are shown in Table 1. We observe that the highest kinetic energy release was associated with the lightest fragment H^+ ($m/q = 1$) followed by H_2^+ ($m/q = 2$), as expected. Differently from formic acid photodissociation results (Boechat-Roberty et al. 2005), extremely fast ionic fragments ($U_0 > 10$ eV), usually associated with dissociation of doubly or multiply-charged ions, were not observed at high photon energies.

The study of the decay of core-excited molecules provides information about the bonding or antibonding nature of the molecular orbitals. Generally, the final electronic states of a core excited molecule are unknown due to the fact that the densities of the states are very high, and the bond distances and angles differ from their ground state configuration. The surface potentials of the ionic states are extremely repulsive. For core excited molecules that dissociate into one charged and one or more neutral fragments, the dissociation is primarily controlled by chemical (non-Coulomb) forces originating from the residual valence electrons of the system (Nenner & Morin, 1996). From Table 1, one can see that the mean kinetic energy release U_0 of some acetic acid fragments increases as the photon energy approaches the C 1s edge (288 eV). This enhancement is due to the repulsive character of the σ^* (π^*) resonance.

3.2. Photodissociation and formation pathways

Acetic acid is one of the simplest carboxylic acids. Its underlying decomposition dynamics (dissociation pathways) have been extensively investigated in the UV range, from both experimental and theoretical points of view. On the basis of the stable products observed in UV photolysis gas-phase of acetic acid, several possible dissociation processes (Fang et al. 2002; Mackie & Doolan 1984; Satio et al. 1990; Blake & Jackson

Table 1. Relative intensities (Partial Ion Yield - PIY) and kinetic energy U_0 release by fragments in the acetic acid mass spectra, as a function of photon energy. Only fragments with intensity > 0.1 % were tabulated. The estimated experimental error was below 10%.

Fragments		PIY (%) / U_0 (eV)						
m/q	Attribution	100 eV	200 eV	287.5 eV	288.3 eV	292 eV	300 eV	310 eV
1	H^+	9.16 / 2.9	14.0 / 2.9	10.5 / 2.9	10.6 / 2.9	13.5 / 3.8	16.6 / 3.8	17.6 / 4.9
2	H_2^+	-	0.59 / 3.0	0.53 / 2.4	0.41 / 1.5	0.58 / 3.6	0.77 / 1.9	0.63 / 3.0
12	C^+	1.98 / 0.24	2.69 / 0.31	2.10 / 0.31	2.08 / 0.24	2.71 / 0.40	3.71 / 0.32	3.66 / 0.50
13	CH^+	3.48 / 0.22	4.47 / 0.22	3.81 / 0.22	3.54 / 0.29	4.20 / 0.29	5.24 / 0.37	4.87 / 0.29
14	CH_2^+; CO^{++}	6.71 / 0.21	7.38 / 0.21	6.60 / 0.21	6.54 / 0.20	6.84 / 0.27	7.71 / 0.20	7.61 / 0.34
15	CH_3^+	13.9 / 0.14	12.6 / 0.19	12.6 / 0.10	12.6 / 0.14	10.9 / 0.09	9.35 / 0.14	9.54 / 0.14
16	O^+	2.19 / 0.13	2.88 / 0.37	2.31 / 0.13	2.29 / 0.23	2.81 / 0.13	3.42 / 0.73	3.28 / 0.63
17	OH^+	2.55 / 0.68	2.81 / 1.14	2.34 / 0.79	2.21 / 1.1	2.91 / 0.35	3.26 / 0.69	2.89 / 1.86
18	H_2O^+	0.61 / 0.27	0.76 / 0.12	0.69 / 0.08	0.56 / 0.05	1.43 / 0.05	1.47 / 0.53	0.60 / 0.11
24	C_2^+	-	0.88 / 0.56	0.63 / 0.35	0.58 / 0.48	1.03 / 0.42	1.50 / 0.25	1.17 / 0.56
25	CHC^+ ?	-	1.14 / 0.40	0.89 / 0.40	0.80 / 0.40	1.07 / 0.40	1.50 / 0.95	1.17 / 0.54
26	CH_2C^+ ?	-	0.87 / 0.27	0.68 / 0.23	0.65 / 0.45	0.84 / 0.33	-	0.77 / 0.58
28	CO^+	1.98 / 0.14	2.72 / 0.30	2.26 / 0.26	2.13 / 0.26	2.69 / 0.26	3.96 / 0.10	3.36 / 0.42
29	COH^+; HCO^+	6.13 / 0.16	6.95 / 0.25	6.32 / 0.21	6.42 / 0.21	6.66 / 0.29	7.15 / 0.17	7.06 / 0.40
30	CH_2O^+; $CH3COOH^{++}$?	1.33 / 0.23	-	0.27 / 0.24	0.55 / 0.05	0.22 / 0.45	-	0.21 / 0.16
31	CH_3O^+ ?	-	1.27 / 0.23	1.42 / 0.33	1.41 / 0.27	1.29 / 0.23	1.43 / 0.07	0.92 / 0.27
40	CCO^+	0.37 / 0.01	0.56 / 0.18	0.54 / 0.21	0.52 / 0.22	0.64 / 0.15	1.15 / 0.18	0.71 / 0.18
41	$CHCO^+$	1.17 / 0.12	1.67 / 0.12	1.41 / 0.14	1.39 / 0.18	1.49 / 0.12	1.78 / 0.05	1.59 / 0.24
42	CH_2CO^+	3.47 / 0.09	3.69 / 0.14	3.70 / 0.14	3.63 / 0.11	3.56 / 0.14	3.21 / 0.07	3.31 / 0.17
43	CH_3CO^+;	18.1 / 0.06	12.4 / 0.07	16.4 / 0.07	16.7 / 0.07	13.6 / 0.07	10.1 / 0.05	10.6 / 0.06
44	CO_2^+;CH_3COH^+	1.31 / 0.03	1.34 / 0.07	1.28 / 0.11	1.34 / 0.11	1.19 / 0.09	1.67 / 0.14	1.28 / 0.11
45	$COOH^+$	15.3 / 0.06	12.4 / 0.08	14.1 / 0.08	14.1 / 0.08	13.1 / 0.05	11.0 / 0.11	9.75 / 0.08
46	$HCOOH^+$	-	-	0.15 / 0.06	0.16 / 0.03	-	-	0.12 / 0.06
60	CH_3COOH^+	8.94 / 0.01	4.73 / 0.01	6.45 / 0.01	6.53 / 0.01	6.03 / 0.01	3.94 / 0.02	3.58 / 0.02
61	$^{13}CH_3COOH^+$	1.13 / 0.02	1.16 / 0.06	1.71 / 0.03	2.26 / 0.03	0.21 / 0.02	-	2.45 / 0.05

1969; Ausloss & Steacie 1955) were suggested:

$$CH_3COOH + h\nu \longrightarrow CH_3CO + OH \quad (3)$$
$$\longrightarrow CH_3 + COOH \quad (4)$$
$$\longrightarrow CH_3CO_2 + H \quad (5)$$
$$\longrightarrow CH_2COOH + H \quad (6)$$
$$\longrightarrow CH_4 + CO_2 \quad (7)$$
$$\longrightarrow CH_2CO + H_2O \quad (8)$$

This was also confirmed by Hunnicutt et al. (1989) using both room-temperature and jet-cooled conditions. The major pathway for acetic acid UV photodissociation is reaction 3. Moreover, the observed isotropic distribution of OH fragments from acetic acid dissociation and the parent molecule fluorescence is indicative of a moderately slow dissociation. Reactions 4 and 5 could also lead to CH_3 + CO + OH products (Hunnicutt et al. 1989).

The behavior of acetic acid in the ice phase under the influence of UV photons was recently studied by Maçôas et al. (2004) in an experimental/theoretical approach. The UV photolysis of the Ar matrix-isolated acetic acid reveals very different products from the gas phase. As a result, 37% of the acetic acid molecules yield methanol (CH_3OH) plus carbon monoxide complexes, 17% yield carbon monoxide complexed with formaldehyde and molecular hydrogen, 20% yield quaternary complexes of two carbon monoxides molecules and two hydrogen molecules and 21% dissociate into carbon dioxide and methane (CH_4). Ketene (CH_2CO), which is the main product of thermal decomposition, was detected only in small amounts ($\leq$ 5%). The CO/CO_2 product ratio is $\sim$ 5.

Bernstein et al. (2004) also studied acetic acid in the ice-phase, using both Ar and water matrices and determined the half-life in a UV radiation field and revealed a relatively low survival of acetic acid (large yield of photoproducts) when compared to other organic molecules, like aminoacetonitrile (H_2NCH_2CN). These experiments demonstrate that organic nitriles (cyanide compounds) survive 5 to 10 times longer exposure to UV photolysis than do the corresponding acids.

The present work shows significative differences between the photoproducts of acetic acid due to low ionizing radiation (UV) and soft X-ray photons. The inner shell photoionization process may produce instabilities in the molecular structure (nuclear rearrangements) leading to dissociation. From Table 1 we determine the main photodissociation pathways from single ionizations in 100-300 eV photon energy range. These photodissociation pathways are shown in Table 2. Only events with greater than 1% yields were considered here. The main dissociation leads to production of CH_3CO^+ due to the bond rupture of OH near the carbonyl.

Herbst & Leung (1986) have presented several pathway syntheses of complex molecules in dense interstellar clouds via gas-phase chemistry models. The authors presented a significant amount of normal ion-molecule reactions including the

ions C^+, C_2^+, CH^+, OH^+, CO^+, CH_2^+, H_2O^+, HCO^+, C_2H^+, CO_2^+, CH_3^+. In another set of reactions they have shown several radiative associations including the ions C^+, CH_3^+, HCO^+ leading to the production of high molecular complexity species. For example, the possible route to interstellar acetaldehyde, involving the HCO^+ ion and methane by

$$HCO^+ + CH_4 \longrightarrow C_2H_5O^+ + h\nu \xrightarrow{e^-} CH_3CHO + H. \quad (9)$$

Combes et al. (1987) have suggested that the gas phase acetone ($(CH_3)_2CO$) present in the Sgr B2 region could be formed by the radiative association reaction between the methyl ion and interstellar acetaldehyde, followed by dissociative recombination with electrons by

$$CH_3CHO + CH_3^+ \rightarrow CH_3COCH_4^+ + h\nu \xrightarrow{e^-} (CH_3)_2CO + H. \quad (10)$$

Other radiative association reactions with the methyl ion could produce the simplest interstellar ether. In this situation, as proposed by Herbst & Leung (1986), the CH_3^+ reacts with methanol, and after dissociative recombination leads to dimethyl ether by

$$CH_3^+ + CH_3OH \rightarrow CH_3OCH_4^+ + h\nu \xrightarrow{e^-} CH_3OCH_3 + H \quad (11)$$

These works point out the importance of the ionic species in the increase of interstellar molecular complexity. In star-forming regions many ions could be produced by the photodissociation of large organic molecules. Therefore, the knowledge of the photodissociation processes and its ion yields plays an essential role in interstellar chemistry.

The absence of more doubly ionized fragments in the PEPICO spectra indicates that the doubly ionized acetic acid dissociates preferentially via charge separation. The dynamics of the doubly and triple ionized acetic acid molecule will be studied in a future publication.

From Table 2 we can see that two of the main photodissociation pathways of acetic acid occurs with the rupture of the C-C bond, releasing CH_3^+ and $COOH^+$ ions, however the yield of $COOH^+$ (12.8%) undergoes little enhancement with respect to CH_3^+ (11.6%). This small excess could be associated with the high stabilization of $COOH^+$ due to charge resonance (charge migration) (Silverstein & Webster 1998) or a possible dissociation of CH_3^+ into minor fragments. Other possibility is that the methyl carbon IP occurs at 291.6, 5 eV less than for the carboxyl carbon (see Robin et al. 1988). As a consequence, the number of resonances to excited orbitals involving the carbon atom in the COOH site is higher than for the other carbon site at photon energies above the IP of the methyl carbon. This scenario could lead to a small preference for the carboxyl carbon during photoelectron excitation/ionization at these energies (and energies somewhat higher) which, after dissociation, retain the charge.

3.3. Absolute photoionization and photodissociation cross sections

The absolute cross section values for both photoionization and photodissociation processes of organic molecules are extremely important as the input for molecular abundances models (Sorrell 2001). In these theoretical model biomolecules are formed inside the bulk of icy grain mantles photoprocessed by starlight (ultraviolet and soft X-rays photons). Its main chemistry route was based on radical-radical reactions followed by chemical explosion of the processed mantle that ejects organic dust into the ambient gaseous medium. For example, the number density of a given biomolecule in a steady state regime of creation and destruction inside a gaseous-dusty cloud is given by

$$N_{Mol} = \frac{\dot{N}_{Mol} n_d}{< \sigma_{ph-d} > I_0} \quad (12)$$

were $\dot{N}_{Mol}$ is the molecule ejection rate which depends mainly on the molecule mass, the properties of the grains and the cloud (see eq. 21 of Sorrell 2001). n_d is the dust space density, I_0 is the flux of ionizing photons (photons cm^{-2} s^{-1}) inside the cloud and $< \sigma_{ph-d} >$ is the average photodissociation cross section in the wavelength range of the photon flux density.

As mentioned by Sorrell (2001), the main uncertainty in this equilibrium abundance model comes from σ_{ph-d}. Therefore the precise determination of σ_{ph-d} of biomolecules is very important to estimate the molecular abundance of those molecules in the interstellar medium. Moreover, knowing the photon dose ϕ and σ_{ph-d} values its is possible to determine the half-life of a given molecule, as discussed by Bernstein et al. (2004).

The photodissociation rates, R, of a molecule dissociated by the interstellar radiation field I_ε in the energy range $\varepsilon_2 - \varepsilon_1$ is given by

$$R = \int_{\varepsilon_1}^{\varepsilon_2} \sigma_{ph-d}(\varepsilon) I_0(\varepsilon) d\varepsilon \quad (13)$$

where $\sigma_{ph-d}(\varepsilon)$ is the photodissociation cross section as a function of photon energy (cm^2), $I_0(\varepsilon)$ is the photon flux as a func-

Table 2. Main photodissociation pathways from single ionization

$CH_3COOH + h\nu$	$\longrightarrow$	$CH_3COOH^+ + e^-$
CH_3COOH^+	$\xrightarrow{14.1\%}$	$CH_3CO^+ + OH$ or $(O + H)$
	$\xrightarrow{13.1\%}$	H^+ + neutrals
	$\xrightarrow{12.8\%}$	$COOH^+ + CH_3$ or $(CH_2 + H)$
	$\xrightarrow{11.6\%}$	$CH_3^+ + COOH$ or $(CO_2 + H; CO + OH)$
	$\xrightarrow{7.1\%}$	$CH_2^+ + HCOOH$ or $(H + COOH)$
	$\xrightarrow{6.7\%}$	$COH^+ + CH_3 + O$
	$\xrightarrow{4.2\%}$	CH^+ + neutrals
	$\xrightarrow{3.5\%}$	$CH_2CO^+ + H_2O$ or $(OH + H)$
	$\xrightarrow{2.7\%}$	$CO^+ + CH_3 + OH$
	$\xrightarrow{2.7\%}$	O^+ + neutrals
	$\xrightarrow{2.7\%}$	$OH^+ + CH_3CO$ or $(CH_3 + CO)$
	$\xrightarrow{1.5\%}$	$CHCO^+$ + neutrals
	$\xrightarrow{1.4\%}$	$CO_2^+ + H + CH_3$ or $(CH_2 + H)$

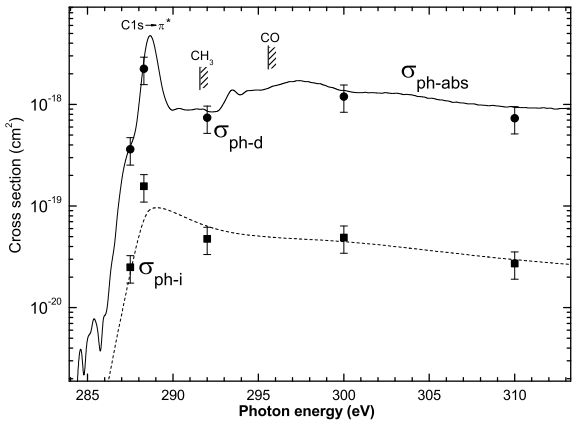

Fig. 5. Non-dissociative single ionization (photoionization) cross section (σ_{ph-i}) and dissociative ionization (photodissociation) cross section (σ_{ph-d}) of acetic acid as a function of photon energy. The photoabsorption cross-section (σ_{ph-abs}) taken from Robin et al. (1988) is also shown.

tion of energy (photons $cm^{-2}eV^{-1}s^{-1}$) (see discussion in Cottin et al. 2003 and Lee 1984).

The half-life may be obtained from Eq. 13 by writing $t_{1/2} = ln2/R$, which does not depend on the molecular number density.

In order to put our data on an absolute scale, after subtraction of the linear background and false coincidences coming from aborted double and triple ionization (see Simon et al 1991), we have summed the contributions of all cationic fragments detected and normalized them to the photoabsorption cross sections measured by Robin et al (1988).

Assuming a negligible fluorescence yield (due to the low carbon atomic number (Chen et al 1981)) and anionic fragments production in the present photon energy range, we adopted that all absorbed photons lead to cationic ionizing process. Therefore the non-dissociative single ionization (photoionization) cross section σ_{ph-i} and the dissociative single ionization (photodissociation) cross section σ_{ph-d} of acetic acid can be determined by

$$\sigma_{ph-i} = \sigma^{+} \frac{PIY_{CH_3COOH^+}}{100} \quad (14)$$

and

$$\sigma_{ph-d} = \sigma^{+}\left(1 - \frac{PIY_{CH_3COOH^+}}{100}\right) \quad (15)$$

where σ^+ is the cross section for single ionized fragments (see description in Boechat-Roberty et al. 2005).

Both cross sections can be seen in Figure 5 as a function of photon energy. The absolute absorption cross section of acetic acid (Robin et al. 1988) is also shown for comparison. Those values are also shown in Table 3.

Table 3. Values of non-dissociative single ionization (photoionization) cross section (σ_{ph-i}) and dissociative ionization (photodissociation) cross section (σ_{ph-d}) of acetic acid as a function of photon energy. The estimated total error is 30%. The photoabsorption cross section (σ_{ph-abs}) from Robin et al. (1988) is also shown.

Photon	Cross Sections (cm^2)		
energy (eV)	σ_{ph-d}	σ_{ph-i}	σ_{ph-abs}
285	3.61×10^{-19}	2.49×10^{-20}	4.12×10^{-19}
288.3	2.23×10^{-18}	1.56×10^{-19}	2.58×10^{-18}
292	7.40×10^{-19}	4.75×10^{-20}	8.52×10^{-19}
300	1.19×10^{-18}	4.89×10^{-20}	1.37×10^{-18}
310	7.32×10^{-18}	2.72×10^{-20}	9.31×10^{-19}

4. Summary and conclusions

The goal of this work was to experimentally study ionization and photodissociation processes of a glycine precursor molecule, CH_3COOH (acetic acid). The measurements were taken at the Brazilian Synchrotron Light Laboratory (LNLS), employing soft X-ray photons from a toroidal grating monochromator (TGM) beamline (100 - 310 eV). The experimental set-up consists of a high vacuum chamber with a time-of-flight mass spectrometer (TOF-MS). Mass spectra were obtained using coincidence techniques.

We have shown that X-ray photon interactions with acetic acid release a considerable number of energetic fragments, some of them with high kinetic energy (ex. H^+, H_2^+ and OH^+). Unlike the previous work with formic acid performed in the same spectral range (Boechat-Roberty et al. 2005), no very high kinetic energy fragments have been observed due the single photoionization of acetic acid.

Several ionic fragments released from acetic acid photodissociation have considerable kinetic energy. An extension of this scenario to interstellar medium conditions suggests the possibility endothermic ion-molecule (or radical-molecule) reactions and this becomes important in elucidating the pathways of formation of complex molecules (Largo et al. 2004).

Dissociative and non-dissociative photoionization cross sections were also determined. We found that about 4-6% of CH_3COOH survive the soft X-ray ionization field. CH_3CO^+ and $COOH^+$ were the main fragments produced by high energy photons. The former may indicate that the production-destruction cycle of acetic acid in hot molecular cores could decrease the H_2O abundance, since the net result of this process is the conversion of water into OH + H. The latter ion plays an important role in ion-molecule reactions to form large biomolecules like glycine.

Acknowledgements. The authors would like to thank the staff of the Brazilian Synchrotron Facility (LNLS) for their valuable help during the experiments. We are particularly grateful to Dr. R. L. Cavasso and Professor A. N. de Brito for the use of the Time-of-Flight Mass Spectrometer. This work was supported by LNLS, CNPq and FAPERJ.

References

Ausloos P. & Steacie E. W. R. 1955, Can. J. Chem., 33, 1530.

Bernstein M. P., Ashbourn S. F. M., Sandford S. A. & Allamandola L. J. 2004, ApJ, 601, 365.

Blake P. G., Jackson G. E., 1969, J. Chem Soc. B, 94.

Boechat-Roberty H. M., Pilling S. & Santos A. C. F. 2005, A&A 438, 915.

Cazaux, S., Tielens, A. G. G. M., Ceccarelli, C., Castets, A., Wakelam, V., Caux, E., Parise, B. & Teyssier, D. 2003, ApJ, 593, L51.

Cardoso E. S. 2001, MSc. thesis, IF/UNICAMP, São Paulo, Brazil.

Chen M. H., Crasemann B. & Mark, H., 1981, Phys. Rev. A, 24, 177.

Combes F., Gerin M., Wooten A. S., et al., 1987, A&A, 180, L13.

Cottin H., Moore M., H. & Bénilan, Y. 2003, ApJ, 590, 874.

Crovisier J., Bockelée-Morvan D. 1999 Space Scien. Rev., 90, 19.

Crovisier J., Bockelée-Morvan D., Colom P., Biver N., Despois D. & Lis D. C. 2004, A&A, 418, 1141.

Ehrenfreund P. & Charnley S. B. 2000, ARA&A, 38, 427.

Fang W.-H., Liu R.-Z., Zheng X. & Phillips D. L. 2002, J. Org. Chem., 67, 8470.

Goicoechea J. R., Rodriguez-Fernandez N. J. & Cernicharo J. 2004 ApJ, 600, 214.

Hansen D. L. et al, 1998, Phys. Rev. A, 58, 5.

Herbst E. & Leung C. M., 1986, MNRAS, 222, 689.

Hollis J. M., Vogel S. N., Snyder L. E., Jewell P. R. & Lovas F. J. 2001, ApJ, 554, L81.

Huntress W.& Mitchell G. 1979, ApJ, 231, 456.

Hunnicutt S. S., Waits L. D. & Guest J. A., 1989, J. Phys. Chem., 93, 5188.

Kuan Y.-J., Charnley S. B., Huang H.-C., Tseng W.-L., Kisiel Z. 2003, ApJ, 593, Issue 2, 848.

Kuan, Y.J., Charnley, S. B., Huang, H.C., Kisiel, Z., Ehrenfreund, P., Tseng, W.L. & Yan, C.H., 2004, Adv. Space Res., 33, 31.

Lago A. F., Santos A. C. F. & de Souza G. G. B. 2004, J. of Chem. Phys., 120, 9547.

Largo A., Redondo P. & Barrientos C. 2004, Int. J. Quant. Chem., 98, 355.

Lee L. C. 1984, ApJ, 282, 172.

Liu S. Y., Girard J. M., Remijan A. & Snyder L. E. 2002, ApJ, 576, 255.

Mackie J. C. & Doolan K. R. 1984, Int. J. Chem. Kinet., 16, 525.

Maçôas A. M. S., Khriachtchev L., Fausto R. & Räsänen M. 2004, J. Phys. Chem., 108, 3380.

Mendoza, C., Ruette, F., Martorell, G., & Rodríigez, L. S. 2004, ApJ, 601, L59.

Mehringer D. M., Snyder L. E. Miao Y. & Lovas F. J. 1997, ApJ, 480, L71.

Naik P. D., Upadhya P. H., Kumar A. Sapre A. V. & Mittal J. P. 2001, Chem. Phys. Letters, 340, 116.

Nenner, I., & Morin, P., 1996, VUV and Soft X-Ray Photoinization, Ed. Uwe Becker and D. A. Shirley, Plenum Press, New York.

Nummelin A., Bergman P., Hjalmarson Å., Friberg P., Irvine W. M., Millar T. J., Ohishi M. & Saito S. 2000, ApJS, 128, 213.

Remijan A. J., Snyder L. E., Liu S.-Y. Mehringer D. & Kuan Y. -J. 2002, ApJ, 576, 264.

Remijan A. J., Snyder L. E., Friedel D. N., Liu S.-Y. & Shah R. Y. 2003, ApJ, 590, 314.

Remijan A. J., Shiao Y. -S., Friedel D. N., Meier D. S. & Snyder L. E. 2004, ApJ, 617, 384.

Robin, M. B., Ishii I., McLaren R. & Hitchcock A. P. 1988, J. Electron Spectrosc. Relat. Phenom., 47, 53.

Santos A. C. F., Lucas C. A. & de Souza G. G. B. 2001, J. Electron Spectrosc. Relat. Phenom., 114, 115.

Satio K., Sasaki T., Yoshinobu I. & Imamura A. 1990, Chem. Phys. Lett., 170, 385.

Silverstein R. M. & Webster F. X., 1998, "Spectrometric Identification of Organic Compounds", 6th edition., John Wiley & sons, Inc.

Simon M., LeBrun T., Morin P., Lavolée M. & Maréchal J. L. 1991, Nucl. Instrum. Methods B, 62, 167.

Snyder L. E., Lovas F. J., Hollis J. M. et al. 2005, ApJ, 619, 914.

Sorrell, W. H. 2001, ApJ, 555, L129.

Sutton E. C., Blake G. A., Masson C. R. & Phillips T. G. 1985, ApJS, 58, 341

Turner B. E. 1991, ApJS, 76, 617.

Wiley W. E., & McLaren I. W. 1955 Rev. Sci. Instrum. 26, 1150.

Wlodarczak G. & Demaiso J. 1988, A&A, 192, 313.

Woon D. E. 2002, ApJ, 571, L177.

Wotten A., Wlodarczak G., Mangnum J. G., Combes F., Encrenaz P. J. & Gerin M. 1992, A&A, 257, 740.